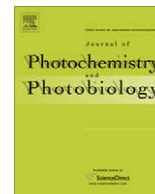




Contents lists available at ScienceDirect

Journal of Photochemistry and Photobiology B: Biology

journal homepage: www.elsevier.com/locate/jphotobiol

Variability in photobleaching yields and their related impacts on optical conditions in subtropical lakes

Steven A. Loiselle^{a,*}, Luca Bracchini^a, Andres Cózar^b, Arduino M. Dattilo^a, Antonio Tognazzi^a, Claudio Rossi^a

^a Environmental Spectroscopy Lab, Dipt. Farmico Chimico Tecnologico, CSGI, University of Siena, via Aldo Moro 1, 53100 Siena, Italy

^b Área de Ecología, Facultad de Ciencias del Mar y Ambientales, Universidad de Cádiz, Campus Río San Pedro. 11510 Puerto Real (Cádiz), Spain

ARTICLE INFO

Article history:

Received 20 May 2008

Received in revised form 30 January 2009

Accepted 9 February 2009

Available online 20 February 2009

Keywords:

CDOM

Photodegradation

Photobleaching

Conservative mixing

Lakes

Argentina

ABSTRACT

Changes in the concentration and spectral absorption of chromophoric dissolved organic matter (CDOM) may strongly condition the optical properties of tropical and subtropical water bodies. We examined the spatial distribution of CDOM-related absorption, spectral slope and vertical attenuation of solar radiation in two shallow lakes in the Esteros del Iberá wetland system. In situ measurements were made to examine spatial variations in photobleaching yields in natural lake conditions. The results showed that “fresh” allochthonous CDOM is more susceptible to phototransformations than either “aged” allochthonous organic matter or autochthonous sources, if the distances from sources are considered as proxies for residence time. Based on measured changes in absorption spectral slope in relation to solar ultraviolet irradiance, a model was developed which used CDOM as a non-conservative tracer of water masses. Spatial changes in CDOM absorption within the lake were then used to compare photo related transformations to those associated with conservative mixing.

© 2009 Elsevier B.V. All rights reserved.

1. Introduction

Solar ultraviolet radiation plays an important role in modifying the chemical and biological environment of aquatic ecosystems [1,2]. Chromophoric dissolved organic matter (CDOM) is a major regulator of these effects. The impacts of CDOM on primary productivity and secondary production and the phototransformation (degradation and bleaching) of dissolved organic matter have recently received much study [3]. The degree of photodegradation (reduction of molecular weight) and photobleaching (loss of absorption in the ultraviolet and visible wavelengths) of CDOM depends on the spectral intensity of the incident irradiance in the water column and the duration of exposure, as well as on CDOM photoreactivity and spectral absorptivity [4]. The photochemical transformation of CDOM results in the production of low molecular weight organic compounds and dissolved inorganic carbon. Consequences for the aquatic ecosystem include the formation of toxic photoproducts [5,6], increase in the pool of bioavailable carbon substrates [7], impacts on secondary productivity, as well as changes in the amount and spectral properties of light in the water column with implications on photosynthesis and productivity.

The photoreactivity of CDOM is strongly influenced by its origin and chemical composition [8,9]. CDOM from terrigenous sources

has been shown to be sensitive to photo-induced degradation, while plankton derived dissolved organic matter appears to be relatively less photoreactive [10,11]. Direct and indirect reactions of plankton derived dissolved organic matter and terrigenous CDOM have also been shown to occur [10]. In many lake environments, several sources of CDOM may be present and the resulting optical heterogeneity will depend upon the proximity to sources, the exposure history, and the degree of mixing between waters containing different types of CDOM.

Recently, a number of important developments in the modeling and understanding of CDOM degradation processes have been made. These studies, using one or more CDOM sources, have compared the changes in the absorption characteristics of CDOM under carefully controlled conditions [9,13,14], providing a basis for the study of optical changes in aquatic ecosystems. One critical aspect of these approaches is that experimental conditions often differ from those in which the CDOM is generated and eventually mineralised. Few systematic studies have addressed the spatial variability of the photodegradation processes across optically different areas of the same ecosystem, or in response to variable conditions of irradiance, pH, salinity and temperature [12,15,33]. Such information could provide insights into carbon cycling, hydrodynamics and effects of climate change on optical conditions.

In the present study, we examine the short term photobleaching yields (changes in absorption magnitude with incident irradiance in the ultraviolet wavelengths) and changes in absorption

* Corresponding author. Tel.: +39 0577 234 360.

E-mail address: loiselle@unisi.it (S.A. Loiselle).

spectral slope for samples obtained from a range of habitats in subtropical wetland lakes. The measured change in absorption spectral slope with increasing incident irradiance are indicative of photo-transformation in CDOM molecular structure (as well changes in other compositional characteristics such as aromaticity [9]). In situ measurements are then compared with lake optical conditions at these same sites to examine trends in the spectral conditions of the water column over time and space. Information on CDOM absorption properties was then compared to modelled impacts of conservative mixing to examine the relative importance of control mechanisms of optical conditions in the study lakes.

2. Materials and methods

2.1. Study sites

Sampling and measurements in two shallow inland lakes in the Esteros del Iberá wetland complex (Argentina) were made in November and December 2006. Laguna Iberá is a shallow humic lake (58 km², average depth 3.1 m) located on the eastern border (latitude 28.5° S, longitude 57.1° W) of the Esteros. The lake presents heterogeneous optical conditions and slowly evolving hydrological conditions, which appear to be sensitive to local environmental change [16,17]. Laguna Iberá receives CDOM rich waters from a wetland lined river to the south (Río Miriñay) [18] and is bordered by a small population centre (Fig. 1). To the north, a small stream brings water from an extensive wetland area, dominated by dense emergent vegetation, into the lake. Laguna Galarza (latitude 28.0° S, longitude 56.7°) is a smaller and shallower lake (16 km², average depth 1.9 m) which presents more homogeneous optical conditions (Fig. 1e). Both lakes present little vertical stratification and are surrounded on several sides by rooted and floating vegetation.

2.2. Methods

Sampling sites (75 sites in total) were selected in Laguna Iberá (65 sites) and Laguna Galarza (10 sites) to include the widest range of previously reported [19,20] optical and biological conditions (Fig. 1a and e). Measurements of absorption properties, vertical diffuse attenuation, chlorophyll-*a* fluorescence and incident solar irradiance were obtained for each site. For a subset of sites (40), changes in CDOM absorption characteristics with cumulative exposure were determined in situ under natural sunlight and lake temperature conditions. These sites were selected to cover most optical conditions reported in previous studies [18,20].

Water samples (2 l) were collected at each site at a depth of 0.5 m for chlorophyll-*a* and CDOM absorption measurements. Reference measurements for spectral absorption and fluorescence were made of the polyethylene sampling bottles using MilliQ water prior to sampling. An aliquot of the sample (0.5 l) was filtered twice with prerinsed Whatman GF/F glassfiber filters and single use 0.22 μm polyethersulfone filters (Milllex GP Filter Unit, Millipore S.A., Malsheim, France) [18]. For the 40 sites for which photodegradation was measured in situ, the filtrate was injected directly into sterile Tedlar (polyvinylfluoride) sampling bags. Prior to injection, bags were examined for the potential release of CDOM using MilliQ water over a period of 24 h. No increase in absorption was observed, allowing us to conclude that the Tedlar sampling bags did not contribute to CDOM absorption or sample bias. The spectral transmission of the Tedlar bags was measured and showed a high transmittance throughout the visible (75%) and UV wavebands (UVB 55%, UVA 65%).

Bags containing filtered lake samples were then placed in a wind sheltered cove on the western part of Lake Iberá (Fig. 1a). Bags were fixed in a horizontal position, just below the surface of

the water (<1 cm depth), to allow a constant movement of lake water around the bags. Samples were exposed from sunrise to sunset for a single day (average 12.5 h). One set of bags was exposed for 1.5 sample days (17.5 h) to compensate for irradiance loss due to clouds. Prior to initiating the experiment, a set of samples (7) from different locations of lake was filtered (0.22 μm) and stored for 12 h in the dark to examine changes in optical properties not related to photodegradation.

Samples (30 ml) were obtained every 4 h from each Tedlar bag after rinsing the external parts with sterilized water. Samples were housed in dark glass containers, covered and stored at 4 °C until analysis.

Absorbance scans were performed using a Lambda 25 spectrophotometer (PES, Perkin Elmer) (scan speed of 4500 nm min⁻¹). A single, acid cleaned, quartz cuvette of 1 cm path length was used. A Milli-Q blank was run before each scan to maintain baseline. After acclimation in a temperature controlled room (18 °C), three scans were performed for each sample and the average absorbance was determined over a wavelength range of 200–800 nm, with a spectral resolution of 1 nm. The average absorbance from 700 nm to 720 nm was subtracted from each measurement to avoid problems related to minimal baseline changes. Absorption coefficients (a_{λ} , m⁻¹) were calculated from absorbance measurements (A_{λ}) at 240, 270, 365 and 440 nm using $a_{\lambda} = 2.303/0.01 \times A_{\lambda}$.

One of the most useful parameters in the characterization of CDOM is the spectral slope, associated with the near exponential decrease in absorption with wavelength. Changes in spectral slope have been related to changes in aromaticity and average molecular weight [21,24–26]. Spectral slope coefficients (S) were estimated [22,23] using a nonlinear fitting technique (Levenberg–Marquardt minimising method) according to:

$$a(\lambda) = a_0 e^{S(\lambda_0 - \lambda)} + k \quad (1)$$

where a_0 is the absorption coefficient at λ_0 (e.g. 270 nm), S (nm⁻¹) is the spectral slope coefficient. The k term is a background parameter near zero, included to examine the goodness of the exponential fit. Spectral slopes were calculated over the spectral region from 270–400 nm ($S_{270-400}$), as slope intervals that extend into the visible wavelengths have been shown to provide little additional information for separating CDOM characteristics. Correlation coefficients between the estimated exponential curve and the measured absorption were found to be greater than 0.99.

Surface irradiance measurements were obtained every minute directly above the lake (1 m) throughout the photodegradation experiment. Multichannel (SKR 1850) and single channel sensors (SKR 420, 430) for ultraviolet A (UVA, 315–380 nm) and ultraviolet B (UVB, 280–315 nm) and visible wavelengths (441 nm, 589 nm, 681 nm, bandwidths 10 nm, 10 nm, 12 nm, respectively) were used (Skye Instruments Ltd., UK). The sensors are cosine corrected with cosine error of 3% for 80°, linearity error <0.2%, absolute calibration error of about 3%, depending on bandwidth channel. The sensor calibration was performed in September 2006, by using a Stellar-Net deuterium lamp (Model #SL3). Dark signal varies from channel to channel and was subtracted. Total incident exposure (KJ m⁻²) was calculated by considering the average solar irradiance in each of the UVB and UVA wavebands [14,15], the total time of exposure and spectral transmission of the Tedlar bags for each waveband weighted for solar spectral irradiance from 280 to 400 nm. Samples within the bags were well mixed due to limited wave action.

At each sampling site in the lake, vertical profiles of solar irradiance (PAR waveband, 305 nm, 340 nm) were measured using a PUV 514 radiometer (Biospherical Instruments, San Diego, CA). Measurements were performed from just below the water surface to near the lake bottom. The profiling radiometer was manually lowered from the sun illuminated side of the boat, obtaining diffuse irradiance measurements every 0.3 s, together with depth.

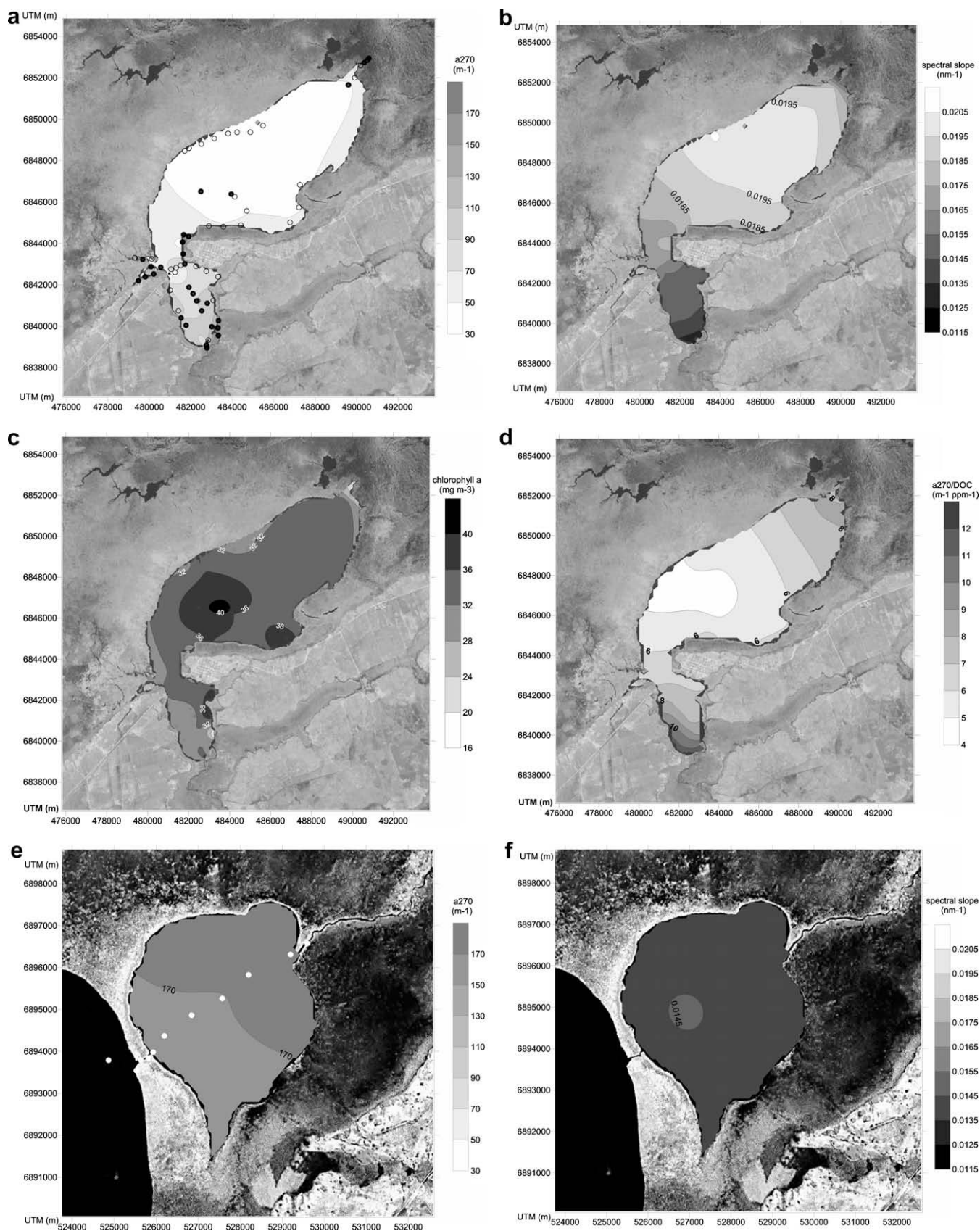


Fig. 1. (a–d): Spatial distribution in Laguna Iberá in November 2006 of; (a) absorption (m^{-1}) at 270 nm, (b) spectral slope (nm^{-1}) from 270–400 nm, (c) chlorophyll-a concentrations (mg m^{-3}), (d) a_{270}/DOC ratio ($\text{m}^{-1} \text{ppm}^{-1}$). (e–f): spatial distribution in Laguna Galarza in November 2006 of (e) absorption (m^{-1}) at 270 nm, (f) spectral slope (nm^{-1}) from 270–400 nm. Sampling sites indicated with open circles. Sites where samples for photodegradation experiments were obtained are indicated with solid circles. Area where in situ photodegradation experiment was performed indicated by grey triangle. Map coordinates are in Universal Transverse Mercator. (g): Calibration curve of fluorescence measurements and measured chlorophyll concentrations (mg m^{-3}) obtained using standard spectrophotometric methods [36].

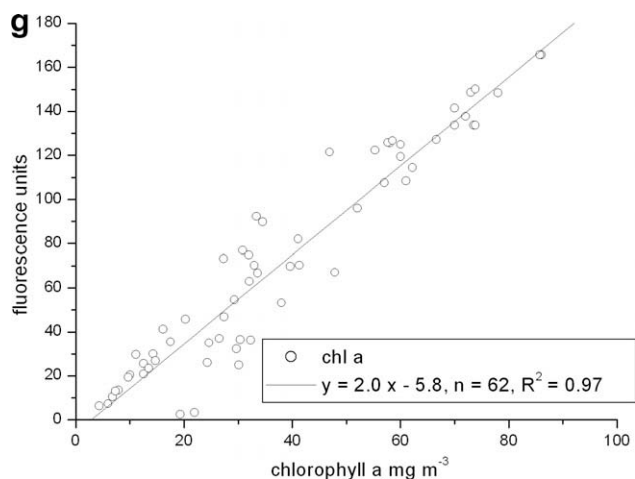


Fig 1. (continued)

On average, 400 measurements (irradiance and water depth) were obtained for each profile. The resulting radiation profile was corrected by removing the dark current signal ($<0.00001 \text{ W m}^{-2} \text{ nm}^{-1}$) and plotted against the water depth. The diffuse attenuation coefficient ($K_{\text{PAR}}, K_{305}, K_{340}$) was calculated by fitting the best exponential curve to the profile data ($E_z = E_0 e^{(-K_z(z-z_0))}$), where irradiance (E_z) over depth (z) follows an exponential decay from the irradiance (E_0) measured just below that lake surface (z_0).

Dissolved organic carbon (DOC) was measured for a subset of samples ($n = 28$) to cover all optical conditions present. The filtered samples were stored in amber glass bottles at 4°C in the dark until the analysis, performed within one week after collection. Measurements were carried out with a Shimadzu 5000 TOC Analyzer equipped with a quartz combustion column filled with 1.2% Pt on silica pillows ($\sim 2 \text{ mm}$ diameter). Samples (10 ml) were acidified with $50 \mu\text{L}$ of 50% H_3PO_4 and sparged for 10 min with CO_2 -free pure air to remove inorganic carbon, before the high temperature catalytic oxidation. The sample was injected in the furnace after a fourfold rinsing using sample water. Measurements were performed in triplicate with a fixed instrumental CV of 2%. A four-point calibration curve was performed by injection of potassium hydrogen phthalate solutions at different concentrations. The system blank was checked on a low-carbon water sample (LCW, $5\text{--}6 \mu\text{M}$). DOC concentrations were calculated [23] and the reliability of measurements was checked daily by using consensus reference materials (CRM) kindly supplied by Prof. D.A. Hansell, University of Miami, USA, consisting of a deep oceanic seawater sample and a LCW (2 CRM and 8 LCW were used per analytical day).

Chlorophyll-*a* concentrations were estimated using a portable fluorometer (excitation wavelength = 485 nm , emission wavelength = 680 nm) which was calibrated daily using a standard solution (SCUFA Submersible Fluorometer, Turner Designs). Fluorometer calibration was made using measurements of chlorophyll-*a* concentrations [sensu Talling and Driver, 27] from different lakes (Fig. 1g) including Laguna Iberá and Laguna Galarza ($n = 19$). Despite of the different sources of variability in the chlorophyll-*a* fluorescence (e.g., quenching, temperature), the measured concentrations and fluorescence signals showed a good linear correlation.

3. Results

CDOM absorption coefficients showed a strong spatial variability, in Laguna Iberá (Fig. 1a) with the highest absorption of the dissolved fraction occurring in the south basin of the lake. The determination of spectral slope ($S_{270\text{--}400}$) showed lowest values in the south and northeastern parts of the lake (Fig. 1b). Phyto-

plankton biomass, estimated using calibrated fluorometer measurements, showed the highest concentrations in the northern basin, and in particular in the north-central area (Fig. 1c). Laguna Galarza showed a more uniform distribution of phytoplankton chlorophyll ($12 \pm 2 \text{ mg m}^{-3}$), spectral slope ($0.0143 \pm 0.0003 \text{ nm}^{-1}$), DOC ($12 \pm 4 \text{ ppm}$) and absorption ($a_{270} = 165 \pm 22 \text{ m}^{-1}$) (Fig. 1e). Shorter residence times and increased resuspension [28] in the smaller and shallower Laguna Galarza may be the principle causes of the higher DOC concentrations and CDOM absorption with respect to Laguna Iberá. Spectral slopes in Laguna Galarza showed little spatial variation (Fig. 1f).

Considering the data from both lakes, CDOM-related absorption showed a negative, but weak correlation with phytoplankton chlorophyll ($r = -0.45$, $p < 0.01$) and turbidity measurements. DOC measurements ($10 \pm 3 \text{ ppm}$, $n = 28$) showed a generally similar spatial pattern as CDOM absorption and were found to be positively correlated with a_{270} ($r = 0.73$, $p < 0.001$).

Changes in absorption characteristics observed during the photodegradation experiments were compared to the cumulative incident irradiance of solar UVB and UVA. The choice to use total UV rather than UVB alone or total insolation was linked to the high reactivity of the chromophores to UV radiation. CDOM of terrestrial origin tends to have a higher reactivity in the UVB wavelengths. However, as photoreactivity of CDOM depends on the reactivity of chromophores and their history of exposure, the larger irradiance of UVA can also play a major role in photobleaching [13]. Cumulative incident exposure [9,14,15] was used to extend photobleaching yields to modelling in-lake processes. It should be noted that total absorbed energy is a more appropriate for the determining of photoreactivity, being more independent of CDOM concentration [12,33]. Cumulative incident irradiance exposure (d , KJ m^{-2}) was determined considering both solar elevation dependent reflectivity (ρ_t) as well as the transmissivity of Tedlar (τ_{Tedlar}) averaged for each waveband (2),

$$d = \int_0^{t_{\text{max}}} (1 - \rho_t) [I_{\text{UVA}_0} \tau_{\text{UVA Tedlar}} + I_{\text{UVB}_0} \tau_{\text{UVB Tedlar}}] dt \quad (2)$$

where I_0 is the incident solar radiation measured above the sampling bags throughout the measurement period ($0 - t_{\text{max}}$). The 40 filtered lake water samples (10 photodegradation experiments each day \times four days) received an average total incident irradiance of 31 KJ m^{-2} (UVB) and 481 KJ m^{-2} (UVA). The time series of spectral absorption measurements of the sample waters showed a reduction in spectral absorption in the UV and short visible wavelengths ($<500 \text{ nm}$). The absolute loss of absorption (Δa_i) with cumulative incident irradiance (d , KJ m^{-2}) depended on the wavelength of interest ($\Delta a_{240}/d > \Delta a_{270}/d > \Delta a_{365}/d > \Delta a_{440}/d$). The degree of loss of absorption varied significantly between sites (Fig. 2a). The relative loss of absorption (normalised by initial absorption and cumulative incident irradiance) showed the highest relative losses at 440 nm and 365 nm (averaging respectively 0.0003 ± 0.0002 and $0.0002 \pm 0.0001 \text{ (KJ m}^{-2}\text{)}^{-1}$), while the relative losses for 240 and 270 were similar ($0.0001 \pm 0.0001 \text{ (KJ m}^{-2}\text{)}^{-1}$) [21]. Samples not exposed to solar radiation did not show significant changes in absorption over the 12 h period ($p > 0.05$, $n = 7$). Spectral slopes showed a significant increase with increasing incident irradiance in all samples (Fig. 2b).

4. Discussion

4.1. Optical measurements

Absorption values measured in both lakes were similar to those reported for humic lakes throughout the world [12,29]. As optical measurements in Laguna Galarza showed limited variability, we focus the following discussion on Laguna Iberá, where clear spatial

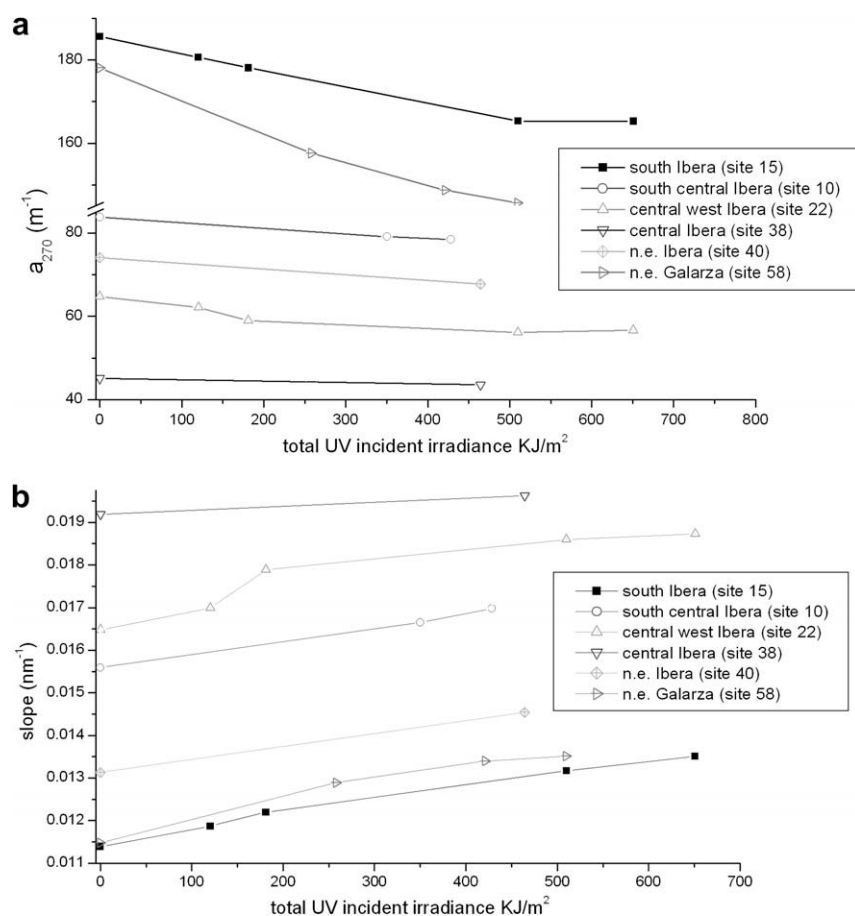


Fig. 2. (a) Reduction in absorption at 270 nm and (b) increase in spectral slope (270–400 nm) due to photodegradation relative to UV incident irradiance (280–315 nm) measured in situ for filtered water samples from Laguna Iberá and Laguna Galarza in November 2006.

trends were observed (Fig. 1a and b). CDOM absorption (a_{240} , a_{270} , a_{365} , a_{440}) was highest in the south and north ends of Laguna Iberá, both areas receiving river waters from extensive wetland areas. Absorption decayed with distance from river inlets to the central area where absorption was minimum.

Phytoplankton biomass presents a potential autochthonous CDOM source, in particular in the center area of Laguna Iberá. Such a source would be expected to produce areas of increased absorption, most likely at 240 nm or 270 nm [30]. The coincident reduction in absorption in both the visible and all UV wavelengths suggests that CDOM distribution throughout the lake is influenced largely by the degradation of allochthonous sources while autochthonous sources may also contribute in a limited manner to the observed CDOM conditions.

Spectral slope measurements confirmed the presence of high molecular weight dissolved organic matter [23,24] entering into the south and north-east parts of the Laguna Iberá. These waters enter into the lake after passing through extensive areas of emergent and floating vegetation, whose thick mats and dense vegetation favour the accumulation of organic detritus [28]. Highly productive, these areas are dominated by *Eichhornia crassipes* and *Scirpus cubensis* and extend for tens to hundreds of kilometres between open lake areas [31]. After entering the south and north basin, spectral slope values increased towards the central basin, indicating an overall reduction in the average molecular weight of the dissolved fraction (Fig. 1b).

Both CDOM absorption and DOC measurements decreased with distance from the river inlets (south and north), with DOC concentrations decreasing comparatively less and in a more variable manner. By normalising absorption (a_{270}) by DOC concentrations, it

was possible to verify the relative loss of chromophores over distance. The large decrease in the a_{270}/DOC ratio (11.5–3.8 $m^{-1} ppm^{-1}$) showed an apparent difference between loss rates of CDOM and DOC (Fig. 1d).

4.2. Photo-induced changes in spectral absorption

A reduction in CDOM absorption may occur through several potential degradation processes as well as through mixing between lake waters with different CDOM characteristics. The in situ incubations were focused on examining changes in spectral absorption due to photodegradation. Microbial activity within the Tedlar bags was minimised by filtering each sample at 0.22 μm . The lack of microbial related activity was confirmed in the dark controls where no significant changes in absorption occurred.

The photobleaching yield was determined by comparing the change in spectral absorption with increasing cumulative incident irradiance. The loss of absorption with respect to incident irradiance followed an exponential-like function [32]. In the lake samples examined, the photobleaching yield was found to be highest where the initial absorption coefficient was largest, in particular near incoming river sources of the allochthonous CDOM. The samples obtained in areas where phytoplankton concentrations were elevated (potential autochthonous CDOM source), and where photodegraded allochthonous CDOM is present, showed a lower photobleaching yield with respect to those areas nearer allochthonous sources (Fig. 3a). It should be noted that those samples with higher initial absorption will absorb more solar energy, likely leading to a higher photobleaching yield. A better approach to examin-

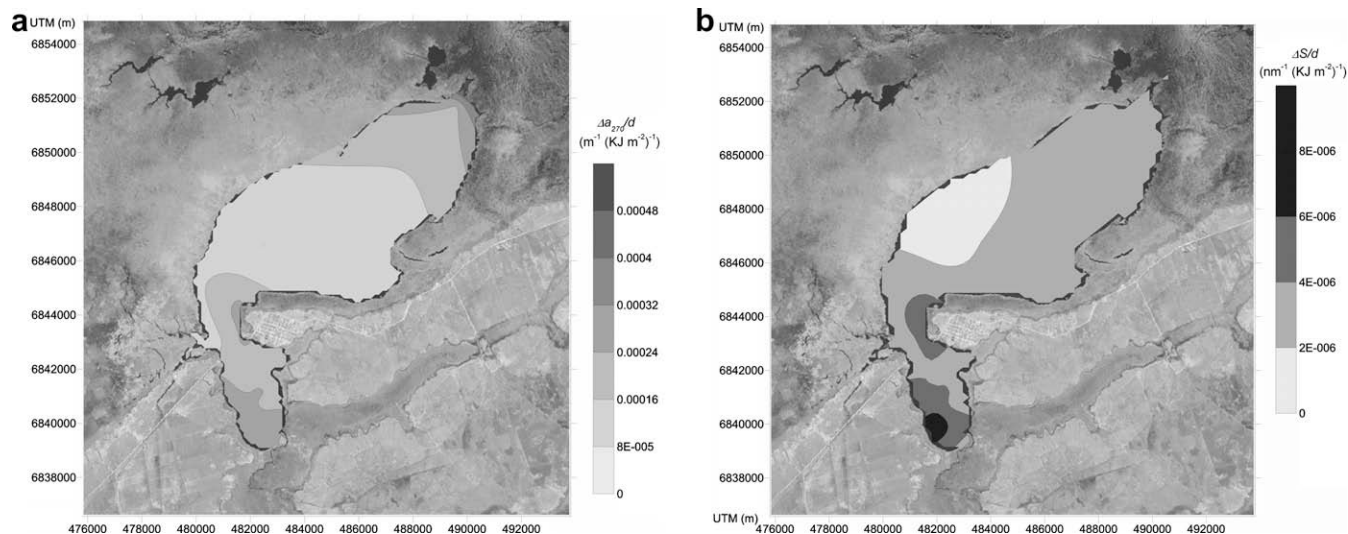


Fig. 3. Spatial distribution of the estimated (a) photobleaching yield (change in absorption at 270 with UV irradiance, $\text{m}^{-1} (\text{KJ m}^{-2})^{-1}$) and (b) change in spectral slope in the spectral band from 270–400 nm with UV irradiance, $\text{nm}^{-1} (\text{KJ m}^{-2})^{-1}$ for Laguna Iberá in November 2006. Sites 10, 15, 22, 28 are shown on the map.

ing the spatial variations in CDOM in relation to incident irradiance is the change in spectral slope.

The change in spectral slope with increasing UV incident irradiance ($\Delta S_{270-400}/d$) was therefore determined (Fig. 2b). Increasing exposure to solar radiation led to an increase in spectral slope in all samples. Previous studies have shown that changes in CDOM absorption spectral slope are indicative of changes in CDOM molecular weight or source (or both) [25,26,34]. The average change in spectral slope was estimated by linearly fitting the spectral slope data over increasing irradiance, and determining the gradient. The degree of change varied according to geographical location (Fig. 3b). The change in the spectral slope was found to be most pronounced where initial absorption was highest and initial spectral slope was lowest. Those samples which displayed the largest $\Delta S_{270-400}/d$ were also found to display the highest photobleaching yield (Fig. 4).

4.3. Spectral slope/absorption ratio

To explore the behaviour of CDOM over time and space, we compared absorption (a_{270}) and spectral slope ($S_{270-400}$) of each

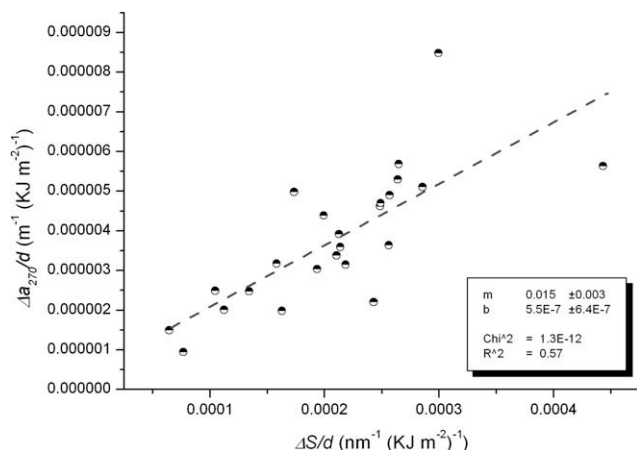


Fig. 4. Relationship between change in absorption at 270 with UV irradiance, $\text{m}^{-1} (\text{KJ m}^{-2})^{-1}$ and the change in S (270–400 nm) with UV irradiance, $\text{nm}^{-1} (\text{KJ m}^{-2})^{-1}$ for samples measured in Laguna Iberá in November 2006. Linear fitting has a correlation coefficient of 0.57 ($n = 25$).

lake sample. For a single CDOM source undergoing photodegradation, the change from high absorption/low slope to low absorption/high slope will appear as a decrease in a $a_{270}/S_{270-400}$ plot (Fig. 5). Where two or more spatially distinct CDOM sources (or sinks) are present, the photodegradation of each CDOM type may be separated, giving a series of overlapping curves with distinct angular coefficients [13]. Within the lake, losses of specific absorption coefficients (e.g. a_{270}) and changes in spectral slope will occur due to degradation processes (photo and microbial) as well as conservative (horizontal) mixing between waters with different absorption properties. In Laguna Iberá, as CDOM moves from the outlet of Rio Miriñay to the south and central basin, the relationship between $S_{270-400}$ and a_{270} changes with distance, decreasing towards a lower absorption and higher spectral slope. The change in position on a $a_{270}/S_{270-400}$ plot shows an exponential decrease with distance from the source (Rio Miriñay) in the south part of the lake (Fig. 6).

While the combined effect of degradation and conservative mixing can be described using the $a_{270}/S_{270-400}$ relationship, it is more difficult to separate the effects of each process. However, using the results of the in situ measurements, we can at least compare the observed change in a_{270} and $S_{270-400}$ in the lake with that

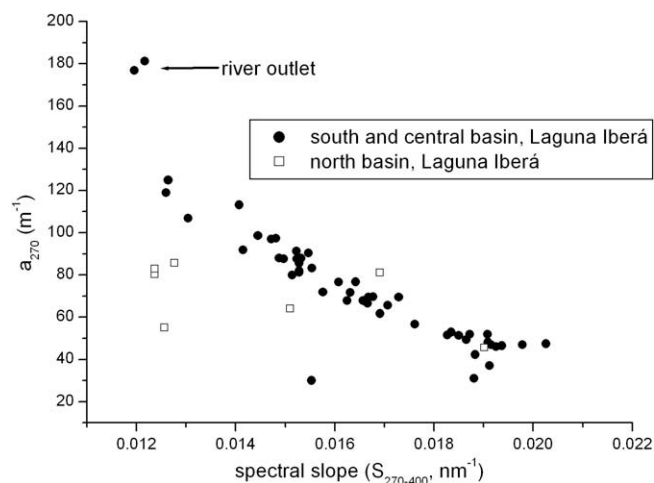


Fig. 5. Measurement of spectral slope ($S_{270-400}$, nm^{-1}) and absorption (a_{270} , m^{-1}) for samples obtained in Laguna Iberá in November 2006.

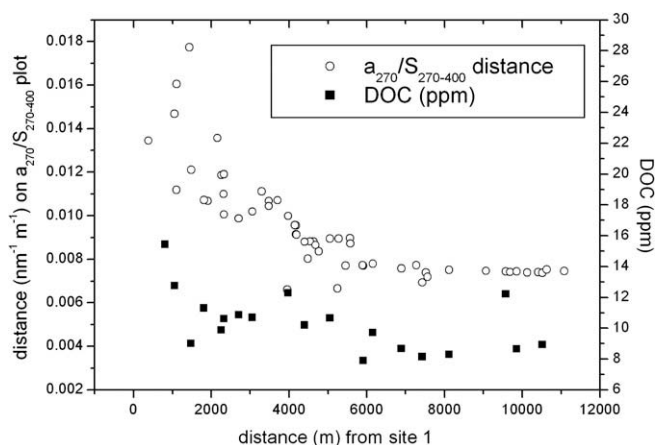


Fig. 6. Relative “distance” in the $a_{270}/S_{270-400}$ graph in relation to source waters (Rio Miriñay) of samples in the south and central basins of Laguna Iberá (open circles, left ordinate) with respect to the physical distance (m) from outlet of Rio Miriñay at the lake border. Measurements of dissolved organic carbon (ppm) also plotted (closed squares, right ordinate).

expected from photodegradation alone and that which would result through conservative horizontal mixing of waters from different areas of the lake.

As demonstrated in Stedmon and Markager [13], conservative mixing between waters with optically different CDOM concentrations will result in changes in a_{270} and $S_{270-400}$ that can be similar to those seen in photodegradation processes. Conservative mixing of “fresh” and “old” CDOM leads to nonlinear changes in the $a_{270}/S_{270-400}$ plot, depending on the degree of mixing ([13] scenarios 1 and 4).

Microbial activities may also influence spectral absorption. While the effects of photodegradation on spectral slope have been demonstrated in this and other studies [25,33], biological degradation presents a more difficult analysis. While some loss of absorption due to biological degradation is expected, studies suggest that only limited changes on spectral slope are likely to occur [9]. However, bacterial degradation of terrestrial DOM which has undergone prior photodegradation has been shown to decrease spectral slope, thus dampening the overall changes in slope due to photobleaching [9].

If changes in the optical properties of CDOM are dominated by photochemical processes, it would be possible to use observed changes in spectral slope with increasing irradiance exposure to model the expected changes in CDOM over time and space. Such conditions occur when the source flowrate dominates water movement (river or narrow bay) and limited horizontal mixing occurs (plug flow). In this situation, changes in spectral slope over distance will depend on “photodegradation yield”, $\Delta S_{270-400}/d$ and overall exposure to solar radiation (photodegradation is more correctly associated with a measured loss of CDOM molecular weight or molecular structure). Measurements of spectral absorption, which are more sensitive to microbial degradation, would be less appropriate.

We examined the spatial distribution in spectral slope within the lake using the $\Delta S_{270-400}/d$ determined in situ ($3.4 \times 10^{-6} \pm 1.8 \times 10^{-6} \text{ nm}^{-1} (\text{KJ}_{\text{UVB} + \text{UVA}} \text{ m}^{-2})^{-1}$), estimated residence times based on measured river flowrates and spatially variable exposure to solar UV radiation. Maximum and minimum flowrates of Rio Miriñay were measured over several days and were within published values [18] of 15,000–29,000 $\text{m}^3 \text{ h}^{-1}$. A simple plug flow model was constructed that used source water (river) flowrates and lake morphology to calculate residence times [35].

To determine the cumulative irradiance of solar UV radiation for water masses at different points in the lake, we used the vertical attenuation measured at 305 nm and 340 nm at each site and the total daily irradiance at the waters surface (I_0 , KJ m^{-2}), corrected for surface reflection. Integrating the exponential decay of solar irradiance (I_{UVB} , I_{UVA}) over lake depth ($z_{\text{mix}} = 3.56 \pm 0.8 \text{ m}$), it is possible to determine the depth integrated daily irradiance exposure to UVB and UVA radiation of each water parcel (3)

$$\int_0^{z_{\text{mix}}} I_{\text{UVB}} dz = \frac{I_0}{(K_{\text{UVB}})} \cdot (1 - e^{-(K_{\text{UVB}})z_{\text{mix}}}) \quad (3)$$

To determine the daily average irradiance exposure throughout the mixing depth, we make several assumptions: a perfectly vertically homogeneous water column, the use of K_{305} and K_{340} as a valid estimate of the vertical diffuse attenuation of the UVB and UVA wavebands, no variability in insolation and optical conditions.

By using the measured $\Delta S_{270-400}/d$, (β , $\text{nm}^{-1} (\text{KJ m}^{-2})^{-1}$), and the calculated daily irradiance (I_{UVB} , I_{UVA} , $\text{KJ m}^{-2} \text{ day}^{-1}$), it is possible to determine the expected change in spectral slope (ΔS) over time. Relating the ΔS with residence time (T_i , day), it is possible to estimate the change of spectral slope over distance, using S as a non-conservative tracer of water masses

$$\Delta S_i = S_{i-1} + T_i \cdot [I_{\text{UVB}} + I_{\text{UVA}}] \cdot \beta_{\text{UVB,UVA}} \quad (4)$$

The results of the model for low and high water flowrates of Rio Miriñay show the expected change of spectral slope over distance (Fig. 7), considering spatial changes both in vertical attenuation and CDOM optical properties. Such a relation has several faults, not the least being that photodegradation is more correctly related to distribution of wavelengths rather than large wavebands. Secondly, the application of a depth integrated daily irradiance to estimate past exposure to solar irradiance assumes that optical conditions in the water column and atmosphere have remained constant. Thirdly, it is unlikely that a plug flow model could appropriately represent water movement in an open lake, where wind forcing and diffusion would play important roles and river discharge will vary over time. Nevertheless, despite the very rough approach of this model, a comparison of changes in spectral slope (modelled and measured) shows reasonable agreement for the south part of the lake and a small part of the center basin. The expected change in spectral slope from pure conservative mixing is also presented. This was determined by using two end members, the a_λ of the source waters (Rio Miriñay) ($a_{270} = 120 \text{ m}^{-1}$, $S_{270-400} = 0.012 \text{ nm}^{-1}$) and the average a_λ of the central part of the lake ($a_{270} = 40 \text{ m}^{-1}$, $S_{270-400} = 0.020 \text{ nm}^{-1}$), together with the relative distance between pools as a proxy for proportions, following the approach of Stedmon and Markager [13]. While it is unlikely that either plug flow or conservative mixing can be used alone to describe spatial variations in CDOM, photodegradation under plug flow conditions shows a reasonable agreement with lake measurements. Such changes in the absorption properties have important implications on radiative transfer and secondary production. This can be clearly seen in the spatial variability of the relative absorption capacity of the dissolved organic compounds (DOC), where a clear reduction occurs over distance (Fig. 8), indicating a change in the relative concentration of chromophores (a_{270}) with distance from the CDOM source (Rio Miriñay). Once again, this change in absorption capacity may be the result of either sinks (eg. photobleaching) or new DOC sources with a low concentration of chromophores. This is further confirmed when the relative change in spectral slope over distance is examined ($S_{270-400}/\text{DOC}$, Fig. 8) indicating a change in average CDOM molecular weight over distance [13,22].

Coloured dissolved organic matter from floating and rooted wetlands strongly modifies the optical conditions and photochemistry in tropical and subtropical inland bodies. The dynamical nat-

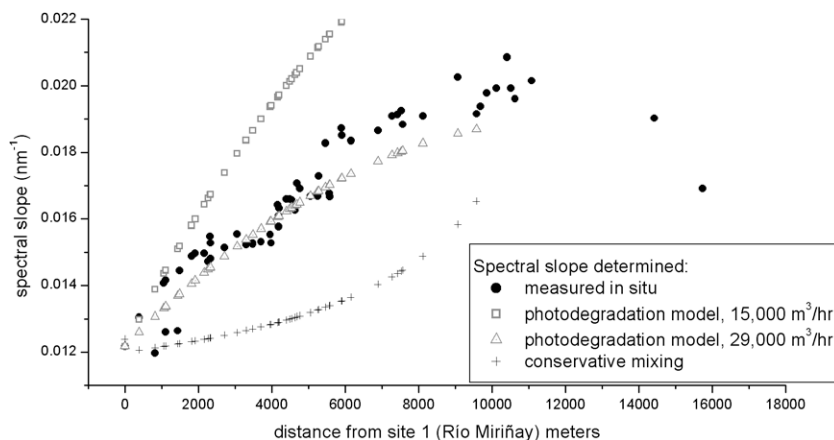


Fig. 7. Measured and modelled change of CDOM spectral slope ($S_{270-400}$, nm^{-1}) over distance in Laguna Iberá. Measurements (solid circles) made in November 2006. Photodegradation model estimates (open squares and triangles) for maximum and minimum flowrates of source waters (Rio Miriñay) considering $\Delta S_{270-400}/d$ determined in situ according to model described in text. Conservative mixing model used measured spectral slopes of source waters and those measured in the central basin.

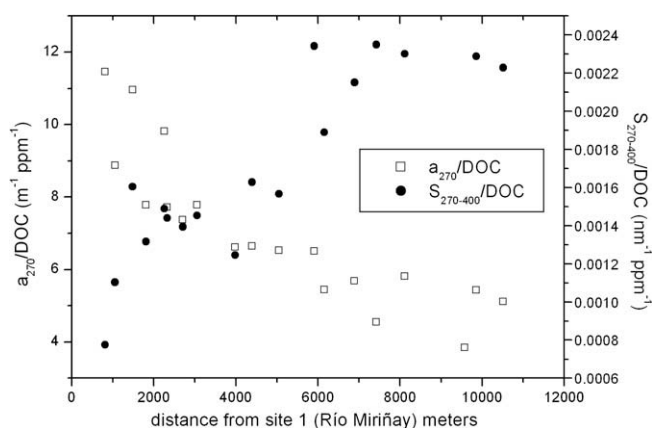


Fig. 8. Changes in the relative absorption and spectral slope normalised by concentration (ppm) of dissolved organic carbon in relation to distance (meters) from source waters (Rio Miriñay) in Laguna Iberá.

ure of these compounds depends upon the spectral quality of solar irradiance within the water column as well as the number and nature of the chromophores present. Combining field measurements and in situ experiments of photodegradation, we show that valuable information regarding the rate of phototransformation of CDOM can be gained and compared to other processes that influence spectral absorption. Furthermore we show how these processes influence the spatial heterogeneity of optical properties. While more information regarding the long term changes in $S_{270-400}$ and a_{270} would improve our understanding of the fate of allochthonous CDOM, this work shows that short term experiments provide new and valuable information on the changing optical properties of these compounds.

Acknowledgements

The present study is conducted under Banco Bilbao Vizcaya Argentaria Foundation sponsored research project entitled IBER-AQUA. We also thank the “Reserva del Iberá” park rangers and particularly Vicente Fraga for their valuable support during the surveys. Funds for this work were also provided by the EU CIRCLE-MED Medcodyn project. The authors gratefully acknowledge the helpful input and comments of Rossana del Vecchio, Chiara Santinelli and anonymous reviewers.

References

- [1] R.G. Zepp, D.J. Erickson, N.D. Paul, B. Sulzberger, Interactive effects of solar UV radiation and climate change on biogeochemical cycling, *Photochem. Photobiol. Sci.* 6 (2007) 286–300.
- [2] D.P. Häder, H.D. Kumar, R.C. Smith, R.C. Worrest, Effects of solar UV radiation on aquatic ecosystems and interactions with climate change, *Photochem. Photobiol. Sci.* 6 (2007) 267–285.
- [3] E.W. Helbling, H.E. Zagarese (Eds.), UV effects in aquatic organisms and ecosystems, *Comprehensive Series in Photochemical and Photobiological Sciences*, The Royal Society of Chemistry, Cambridge, 2003, p. 575.
- [4] S. Bertilsson, L.J. Tranvik, Photochemical transformation of dissolved organic matter in lakes, *Limnol. Oceanogr.* 43 (2007) 753–762.
- [5] C.L. Osburn, D.P. Morris, Photochemistry of chromophoric dissolved organic matter in natural waters, in: E.W. Helbling, H. Zagarese (Eds.), UV Effects in Aquatic Organisms and Ecosystems, The Royal Society of Chemistry, Cambridge, 2003, pp. 185–217.
- [6] R.G. Zepp, Solar ultraviolet radiation and aquatic biogeochemical cycles, in: E.W. Helbling, H. Zagarese (Eds.), UV Effects in Aquatic Organisms and Ecosystems, The Royal Society of Chemistry, Cambridge, 2003, pp. 137–184.
- [7] S. Bertilsson, L.J. Tranvik, Photochemically produced carboxylic acids as substrates for freshwater bacterioplankton, *Limnol. Oceanogr.* 43 (1998) 885–895.
- [8] A. Vodacek, M.D. DeGrandpre, E.T. Peltzer, R.K. Nelson, N.V. Blough, Seasonal variation of CDOM and DOC in the Middle Atlantic Bight: terrestrial inputs and photooxidation, *Limnol. Oceanogr.* 42 (1997) 674–686.
- [9] M.A. Moran, W.M. Sheldon, R.G. Zepp, Carbon loss and optical property changes during long term photochemical and biological degradation of estuarine dissolved organic matter, *Limnol. Oceanogr.* 45 (2000) 1254–1264.
- [10] R. Benner, Chemical composition and reactivity, in: D.A. Hansell, C.A. Carlson (Eds.), *Biogeochemistry of Marine Dissolved Organic Matter*, Academic Press, 2002.
- [11] L.J. Tranvik, S. Kokalj, Decreased biodegradability of algal DOC due to interactive effects of UV radiation, *Aquat. Microb. Ecol.* 14 (1998) 301–307.
- [12] C.L. Osburn, H.E. Zagarese, D.P. Morris, B.R. Hargreaves, W.E. Cravero, Calculation of spectral weighting functions for the solar photobleaching of chromophoric dissolved organic matter in temperate lakes, *Limnol. Oceanogr.* 46 (2001) 1455–1467.
- [13] C.A. Stedmon, S. Markager, Behaviour of the optical properties of coloured dissolved organic matter under conservative mixing, *Estuar. Coast. Shelf S.* 57 (2003) 973–979.
- [14] S. Opsahl, R. Benner, Photochemical reactivity of dissolved lignin in river and ocean waters, *Limnol. Oceanogr.* 43 (1998) 1297–1304.
- [15] E.C. Minor, J. Pothén, B.J. Dalzell, H. Abdulla, K. Mopper, Effects of salinity changes on the photodegradation and UV-visible absorbance of terrestrial dissolved organic matter, *Limnol. Oceanogr.* 51 (2006) 2181–2186.
- [16] L. Bracchini, S.A. Loiselle, S. Mazzuoli, A.M. Dattilo, C. Rossi, Modelling the components of the vertical attenuation of ultraviolet radiation in a shallow lake ecosystem, *Ecol. Modell.* 186 (2005) 43–54.
- [17] R. Ferrati, G.A. Canziani, Analysis of water level dynamics in Esteros del Iberá wetland, *Ecol. Modell.* 186 (2005) 3–16.
- [18] S. Mazzuoli, L. Bracchini, S.A. Loiselle, C. Rossi, An analysis of the spatial and temporal variation evolution of humic substances in a shallow lake ecosystem, *Acta Hydrochim. Hydrobiol.* 31 (2003) 461–468.
- [19] A. Cózar, C.M. Garcia, J.A. Galvez, Analysis of plankton size spectra irregularities in two subtropical shallow lakes (Esteros del Iberá, Argentina), *Can. J. Fish. Aquat. Sci.* 60 (2003) 411–420.

- [20] S.A. Loiselle, L. Bracchini, A. Cozar, A.M. Dattilo, C. Rossi, Examining the spatial distribution of the light environment in a neotropical shallow lake, *Hydrobiologia* 534 (2005) 181–191.
- [21] W. Grzybowski, Effect of short-term irradiation on the absorbance spectra of the chromophoric organic matter dissolved in the coastal and riverine waters, *Chemosphere* 40 (2000) 1313–1318.
- [22] S. Markager, W.F. Vincent, Spectral light attenuation and absorption of UV and blue light in the natural waters, *Limnol. Oceanogr.* 45 (2000) 642–650.
- [23] R. Del Vecchio, N.V. Blough, Photobleaching of chromophoric dissolved organic matter in natural waters: kinetics and modelling, *Marine Chemistry* 78 (2002) 231–253.
- [24] J.R. Helms, A. Stubbins, J.D. Ritchie, E.C. Minor, D.J. Kieber, K. Mopper, Absorption spectral slopes and slope ratios as indicators of molecular weight, source and photobleaching of chromophoric dissolved organic matter, *Limnol. Oceanogr.* 53 (2008) 955–969.
- [25] Y.P. Chin, G. Aiken, E. Oloughlin, Molecular weight, polydispersity, and spectroscopic properties of aquatic humic substances, *Environ. Sci. Technol.* 28 (1994) 1853–1858.
- [26] K.L. Carder, R.G. Steward, G.R. Harvey, P.B. Ortner, Marine humic and fulvic acids: their effects on remote sensing of ocean chlorophyll, *Limnol. Oceanogr.* 34 (1989) 68–81.
- [27] J.F. Talling, D. Driver, Some problems in the estimation of chlorophyll-a in phytoplankton, in: *Proc. Conference of Productivity Measurements, Marine and Freshwaters*, 1961. University of Hawaii, Hawaii, (1963) pp. 142–146.
- [28] A. Cozar, J.A. Gálvez, V. Hull, C. García, S.A. Loiselle, Sediment resuspension by wind in a shallow lake of Esteros del Iberá (Argentina): a model based on turbidimetry, *Ecol. Modell.* 186 (2005) 63–76.
- [29] J.T.O. Kirk, *Light and Photosynthesis in Aquatic Ecosystems*, Cambridge Press, Cambridge, 1994. 401 pp.
- [30] D.M. McKnight, E.D. Andrew, G.R. Aiken, S.A. Spaulding, Aquatic fulvic acids in algal rich Antarctic ponds, *Limnol. Oceanogr.* 39 (1994) 1972–1979.
- [31] P. Gantes, A. Sánchez Caro, F. Momo, M.A. Casset, A. Torremorel, An approximation to the nitrogen and phosphorus budgets in floating soils of a subtropical peatland (Iberá, Argentina), *Ecol. Modell.* 186 (2005) 77–83.
- [32] I. Obernosterer, R. Benner, Competition between biological and photochemical processes in the mineralization of dissolved organic carbon, *Limnol. Oceanogr.* 49 (2004) 117–124.
- [33] M. Tzortziou, C. Osburn, P. Neale, Photobleaching of dissolved organic material from a tidal marsh-estuarine system of the Chesapeake Bay, *Photochem. Photobiol.* 83 (2007) 782–792.
- [34] C.A. Stedmon, S. Markager, The optics of chromophoric dissolved organic matter (CDOM) in the Greenland Sea: an algorithm for differentiation between marine and terrestrially derived organic matter, *Limnol. Oceanogr.* 46 (2001) 2087–2093.
- [35] S.R. Rinaldi, R. Soncini-Sessa, H. Stehfest, H. Tamura, *Modeling and Control of River Quality*, McGraw Hill, New York, NY, 1979.
- [36] J.D. Strickland, T.R. Parsons, *A Practical Handbook of Seawater Analysis*, Fishery Research Board, Canada, 1972.